THE ASTROPHYSICAL JOURNAL, 557:226–239, 2001 August 10

HYDROGEN RECOMBINATION LINES NEAR 327 MHz. III. PHYSICAL PROPERTIES AND ORIGIN OF THE LOW-DENSITY IONIZED GAS IN THE INNER GALAXY

D. ANISH ROSHI
National Centre for Radio Astrophysics, Tata Institute of Fundamental Research, Pune, India; National Radio Astronomy Observatory, Green Bank, WV 24944; aroshi@nrao.edu[1]

AND

K. R. ANANTHARAMAIAH
Raman Research Institute, Sadashivanagar, Bangalore 560 080, India; National Radio Astronomy Observatory, Soccoro, NM 87801-0387; anantha@rri.res.in

Received 2000 September 25; accepted 2001 March 30

ABSTRACT

We present constraints on the physical properties of the ionized gas responsible for hydrogen radio recombination lines (RRLs) near 327 MHz detected in a recent Galactic plane survey made with the Ooty Radio Telescope. To obtain these constraints, we combined the data at 327 MHz with previously published RRL observations near 1.4 GHz. The density of the ionized gas is well constrained and is in the range of 1 to 10 cm^{-3}. The data implies upper limits to the temperature and size of the line emitting regions of $\sim$12,000 K and $\sim$500 pc, respectively. Assuming an electron temperature of 7000 K, the derived path lengths of the line emitting region are in the range of 20 to 200 pc. The derived properties of the ionized gas responsible for the RRL emission near 327 MHz suggest that most of the [N II] 205 μm emission and a considerable fraction of the [C II] 158 μm emission observed in the Galactic plane by the *COBE* satellite could also originate in the same gas. The Hα emission from these ionized gases is mostly undetected in the existing Hα surveys because of large interstellar extinction. About 50% of the free-free absorption of the Galactic nonthermal radiation observed at frequencies less than 100 MHz can be accounted for by the same ionized gas. We also discuss the origin of this low-density ionized gas in the inner Galaxy. The derived low line-of-sight filling factor (<1%) for this ionized gas indicates that it does not form a pervasive medium. On the basis of the similarity of the distribution of this gas in the Galactic disk with that of the star-forming regions and the range of derived physical properties, we support the earlier suggestion that the low-frequency RRL emission originates from low-density ionized gas, which forms envelopes of normal H II regions.

Subject headings: Galaxy: general — H II regions — ISM: clouds — ISM: general — ISM: structure — radio lines: ISM

1. INTRODUCTION

The Galactic disk contains several forms of ionized gas. At the one extreme, there are the two types of widely distributed ionized gases with very low average density that are a part of the general interstellar medium; the warm ionized medium (WIM) with $T_e \sim 10^4$ K and $\langle n_e \rangle > \sim 0.03$ cm^{-3} and the hot ionized medium (HIM) or the coronal gas with $T_e \sim 10^6$ K and $\langle n_e \rangle > \sim 0.03$ cm^{-3} (McKee & Ostriker 1977; Kulkarni & Heiles 1988). The volume filling factor of these components in the ISM is large ($f \sim 0.2$–0.7). At the other extreme are the ultracompact H II regions with $n_e > 10^4$ cm^{-3} and sizes $\ll 1$ pc that are formed around young, hot stars (Wood & Churchwell 1989). Between these two extremes, there are a variety of H II regions over a wide range of densities ($n_e \sim$ 1–1000 cm^{-3}) and a relatively narrow range of temperatures ($T_e \sim$ 3000–10,000 K). The sizes of these regions range from a few parsecs to few tens of parsecs. Somewhere between the two extremes mentioned above, there also appears to be a low-density extended ionized component in the inner Galaxy. This component has been referred to as "extended low-density" (ELD) ionized gas by Mezger (1978) and as "extended low-density warm ionized medium" (ELDWIM) by Petuchowski & Bennett (1993), Heiles (1994), and Heiles, Reach, & Koo (1996b).

Observationally, the low-density extended ionized medium in the inner Galaxy was identified through the detection of radio recombination lines (RRLs) at several positions along the Galactic plane that are free of discrete continuum sources (Gottesman & Gordon 1970; Gordon & Cato 1972). Subsequently, this low-density component has been systematically observed in RRLs near 1.4 GHz by Hart & Pedlar (1976b), Lockman (1976, 1980), Cersosimo (1990), and Heiles et al. (1996b). Recombination lines from this gas was also observed by Anantharamaiah (1985a, 1985b) near 325 MHz. One general result of these observations is that RRLs at $\nu < 1.4$ GHz are detected at almost all the observed positions in the inner Galactic plane ($|l| < 80°$). Recently, new extensive observations of this low-density ionized component in radio recombination lines at frequencies near 327 MHz were made by Roshi & Anantharamaiah (2000, 2001; hereafter Paper I and Paper II) using the Ooty Radio Telescope. From the theory of RRLs, it can be shown that RRLs at low frequencies (<1 GHz) do not originate in normal high-density H II regions because of the effects of continuum opacity, pressure broadening, and beam dilution (Shaver 1975). Observations of low-frequency RRLs are therefore sensitive to relatively low density ($0.5 < n_e < 50$ cm^{-3}), large angular sized (tens of arcminutes) ionized regions.

[1] The National Radio Astronomy Observatory is a facility of the National Science Foundation operated under cooperative agreement by Associated Universities, Inc.

The detection of low-frequency RRLs from almost all the observed positions in the Galactic longitude range 0° to 40° has led to different suggestions for the origin of the low-density gas. For example, Matthews, Pedlar, & Davies (1973) and Shaver (1976) have suggested that they are large, evolved low-density H II regions. On the other hand, Anantharamaiah (1986) has argued that this low-density gas is simply the outer envelopes of the normal (usually higher density) H II regions. Based on the ubiquity of the RRL emission in the inner Galaxy as seen in their recent observations, Heiles et al. (1996b) have associated the lines with the ELDWIM, which they picture as a higher density version of the local WIM. Heiles et al. (1996b) also suggest that about 17% of the low-frequency emission arises in wormlike structures that are the walls of cavities blown by clustered supernova and ionized by hot stars in the same cluster.

To understand the extended low-density ionized gas in the inner Galaxy, it is essential to determine the distribution of the gas in the Galactic plane and compare it with that of other components of the ISM. It is also essential to determine the physical properties of the ionized gas. Information about the angular extent of line emitting regions is needed for determining the physical properties. A study of the distribution of RRL emission in the Galactic disk and comparison with other components were presented in Paper I. The angular extent of the line emitting region is studied by making RRL observations near 327 MHz with a $2° \times 6'$ beam (Paper II). This paper presents constraints on the physical properties of the ionized gas responsible for RRL emission near 327 MHz in the inner Galaxy ($l = 332°$ to 0° to 89°) by combining the data presented in Paper I and the results of Paper II with other existing observations. A brief summary of the data used for the analysis is presented in § 2. Section 3 describes the derivation of the physical properties using the data and a simple model. In § 4, the derived parameters are used to estimate the expected [C II] 158 μm, [N II] 205 μm, and Hα line intensities and the free-free absorption of the Galactic nonthermal emission near 34.5 MHz caused by this gas. The estimated values are then compared with published observations. Section 5 discusses the possible origin of the low-density ionized gas. Section 6 summarizes the paper.

2. SUMMARY OF OBSERVATIONS AND BASIC RESULTS

The RRL surveys, which were described in detail in Papers I & II, were made using the Ooty Radio Telescope (ORT). ORT is a 530 m × 30 m parabolic cylinder operating at a nominal center frequency of 327 MHz (Swarup et al. 1971). The observations were made with two different angular resolutions—$2° \times 2°$ (low-resolution survey) and $2° \times 6'$ (higher resolution survey). A part of the ORT, called a "module," was used for the low-resolution survey, which is described in Paper I. The higher resolution survey was made with the full telescope and is described in Paper II.

In the low-resolution survey, 51 positions were observed in the inner Galaxy: longitude range $l = 332°$ to 0° to 89° and $b = 0°$. The positions were separated in longitude by $\sim 2° \times \sec(\delta)$, δ being the declination. RRLs of hydrogen were detected in ~80% of the observed positions. In the outer Galaxy ($172° < l < 252°$), a total of 14 positions, spaced by ~5°–7° in longitude, were observed. Only three out of these 14 observed positions yielded marginal detection of hydrogen lines. At two specific longitudes in the inner Galaxy ($l = 0.^{\circ}0$ and $13.^{\circ}9$), spectra were taken in steps of 1° up to $b = \pm 4°$ to study the latitude extent of the ionized gas. These observations detected hydrogen lines up to $b \sim \pm 3°$. The observed line profiles and line and continuum parameters have been presented in Paper I. Seven 2° wide fields and two 6° wide fields in the inner Galaxy were observed in the higher resolution survey with the $2° \times 6'$ beam. RRLs were detected in almost all the individual positions within the fields with $l < 35°$ and at several individual positions within the fields in the longitude range $l = 35°$ to 85°. These observations and results are presented in Paper II.

In addition to the RRL data near 327 MHz presented in Papers I & II, RRLs near 1.4 GHz were observed earlier at intervals of 1° in the inner Galaxy by Lockman (1976, 1980) and Hart & Pedlar (1976b) and more recently at finer intervals and also at higher Galactic latitudes by Heiles et al. (1996b). Near $l = 335°$, RRLs were observed at this frequency by Cersosimo (1990). In Paper I, these observations were used to study the distribution of the ionized gas in the inner Galaxy. The similarity of the l-v diagram and the radial distribution of the RRL emission near 327 MHz and 1.4 GHz (Paper I) suggests that they originate from the same ionized regions. The widespread detection of RRLs near 1.4 GHz in the inner Galaxy and the detection of lines at positions where there are no strong continuum sources also supports the fact that they originate from extended regions which the 327 MHz observations are sensitive to (Hart & Pedlar 1976b; Lockman 1976, 1980; Cersosimo 1990; Heiles et al. 1996b). To our knowledge, no other RRL observations are available that can be considered to originate from the same regions. Upper limits on hydrogen line intensity near 75 MHz were available from the data of Erickson, McConnell, & Anantharamaiah (1995). These observations were limited to the longitude range ±20° about the Galactic center.

3. PHYSICAL PROPERTIES OF THE LINE EMITTING REGIONS

The intensity of recombination lines at different frequencies is determined by the physical properties of the ionized gas emitting the lines and the intensity of the background radiation. The physical properties of interest are the electron temperature, the electron density, and the size of the region. These quantities are evaluated from RRL data by computing the expected line emission as a function of frequency based on a simple model and comparing them with the observed values.

3.1. *A Simple Model*

We consider a single homogeneous ionized cloud embedded in the Galactic nonthermal background radiation field. The line intensity from such a cloud can be obtained by solving the radiative transfer equation. The line brightness temperature $T_{\rm LB}$, which is the excess temperature above the continuum temperature, can be written as (Shaver 1975)

$$T_{\rm LB} = T_{0{\rm bg},\nu} e^{-\tau_{{\rm C}\nu}} (e^{-\tau_{{\rm L}\nu}} - 1) + T_e \left\{ \frac{b_m \tau^*_{{\rm L}\nu} + \tau_{{\rm C}\nu}}{\tau_{{\rm L}\nu} + \tau_{{\rm C}\nu}} [1 - e^{-(\tau_{{\rm L}\nu} + \tau_{{\rm C}\nu})}] - (1 - e^{-\tau_{{\rm C}\nu}}) \right\} + T_M \left[\frac{1 - e^{-(\tau_{{\rm L}\nu} + \tau_{{\rm C}\nu})}}{\tau_{{\rm L}\nu} + \tau_{{\rm C}\nu}} - \frac{(1 - e^{-\tau_{{\rm C}\nu}})}{\tau_{{\rm C}\nu}} \right], \quad (1)$$

where $T_{0bg,\nu}$ is the temperature of the Galactic background

radiation incident on the cloud, T_e is the electron temperature of the ionized gas, T_M is the temperature of the background radiation intensity within the cloud and $\tau_{C\nu}$ is the continuum optical depth. The non-LTE line optical depth of the spectral transition from energy state m to n is $\tau_{L\nu}$. $\tau_{L\nu} = b_n \beta_n \tau^*_{L\nu}$, where $\tau^*_{L\nu}$ is the LTE line optical depth. b_n and β_n are the departure coefficients of state n and are defined as

$$b_n \equiv \frac{N_n}{N_n^*}, \tag{2}$$

$$\beta_n \equiv \frac{(1 - (b_m/b_n)e^{-E_{nm}/kT_e})}{(1 - e^{-E_{nm}/kT_e})}$$

$$\approx 1 - \frac{d[ln(b_n)]}{dn} \Delta n \frac{kT_e}{h\nu}. \tag{3}$$

Here N_n^* and N_n represents the atomic level population of the state n in LTE and non-LTE, respectively, E_{nm} is the energy difference between states m and n and $\Delta n = m - n$. In equations (1) and (3), b_m is the departure coefficient for state m. Assuming that the Galactic background emission extends over a line-of-sight distance D_{bg} (i.e., the extent of the Galactic disk along the line of sight) with uniform emissivity, $T_{0bg,\nu}$ and T_M are obtained as follows:

$$T_{0bg,\nu} \approx \frac{T_{bg,\nu}}{D_{bg}} (D_{bg} - D_c), \tag{4}$$

$$T_M \approx \frac{T_{bg,\nu}}{D_{bg}} S, \tag{5}$$

where $T_{bg,\nu}$ is the observed Galactic background temperature, and S is the size of the ionized gas. D_c is the distance to the ionized gas, which can be obtained from the observed central velocity of RRLs if we make the standard assumption that the observed central velocity is caused by differential Galactic rotation. The observed line temperature T_{LA} is related to the computed brightness temperature as

$$T_{LA} = \frac{\Omega_{cloud}\eta_B}{\Omega_B} T_{LB}, \tag{6}$$

where Ω_{cloud} is the solid angle of the cloud, Ω_B is the half-power beam solid angle of the telescope and η_B is the main-beam efficiency.

Using the above equations and the observed line parameters, it is possible, in principle, to constrain the physical properties of the ionized gas. Since the line intensity depends on more than one parameter, better constraints are obtained if RRL observations from the same ionized gas are available at different frequencies. Sections 3.4 and 3.5 combine our 327 MHz observations with those near 1.4 GHz and 75 MHz to constrain the physical properties of the ionized gas (see also § 2). In the models presented in this paper, the line emission is assumed to originate from a single homogeneous ionized region characterized by an electron temperature T_e, density n_e, and size S. Although this is an oversimplification, the available data does not warrant any more details about the regions.

3.2. *Angular Extent of the Line Emitting Region*

The angular extent (Ω_{cloud}) of the ionized region is not determined observationally because of the coarse angular resolution. This parameter is required to estimate the line brightness temperature from the observed line antenna temperature to compare with the prediction by the model (see eq. [6]). The data presented in Paper I indicate that the angular extent of the cloud may be smaller than the beam ($\sim 2^\circ \times 2^\circ$), at least in some cases: the line intensity and the line profile changes significantly from one position to another, which are separated by about 2° in longitude. Along the Galactic latitude, we have observations only at two specific longitudes ($l = 0\overset{\circ}{.}0$, $13\overset{\circ}{.}9$). These observations indicate that the line emission is extended in b over $\sim 1\overset{\circ}{.}8$ (FWHM) (Paper I). However, an examination of the line profiles at different latitudes at $l = 0^\circ$ shows that the profile changes when the beam center is shifted by $\pm 1^\circ$ along b. These changes indicate that the emission from an individual ionized region may have an angular extent less than 2° along Galactic latitude. However, at $l = 13\overset{\circ}{.}9$, the line emission appears to extend beyond $\pm 1^\circ$ along b. Higher angular resolution ($\sim 2^\circ \times 6'$; Paper II) observations toward some of the positions show that the line emitting region may have an angular extent greater than 1°. Based on these observational facts, we assume a cloud size of $\sim 1\overset{\circ}{.}5$ (along b) × 2° (along l). The correction factor $\Omega_B/\Omega_{cloud}\eta_B$ for observations near 327 MHz ($\Omega_B = 2\overset{\circ}{.}2$ [along north-south] × $2\overset{\circ}{.}3$ [along east-west] at declination 0°) is then ~ 2.6. Here we have used the measured main-beam efficiency factor of 0.65 for the telescope. Since the beamwidth of the ORT is a function of declination, the factor $\Omega_B/\Omega_{cloud}\eta_B$ will be different for different directions. Ω_B for a "module" of the ORT has a sec (δ) dependence for $|\delta| < 33^\circ$ and sec^2 (δ) for $|\delta| > 33^\circ$, where δ is the declination.

3.3. *Distance to the Line Emitting Region*

Another unknown quantity is the distance to the ionized region, which is required to estimate the background radiation intensity at its position (see eq. [4]). For modeling presented here, we considered both the "far" and "near" distances based on the observed central velocity of line emission and the rotation curve given by Burton & Gordon (1978) after scaling to $R_\odot = 8.5$ kpc and $\theta_0 = 220$ km s^{-1} (Kerr & Lynden-Bell 1986). Nearer the Galactic center ($|l| < 4^\circ$), the peculiar motion of the ionized gas can dominate over the Galactic differential velocity; hence, the kinematic distance estimate is not reliable. For lack of a better strategy, the ionized gas is assumed to be at half the distance to the Galactic center at these longitudes. The background radiation temperature at the location of the ionized region is then obtained by using the distance to the ionized region, the measured continuum temperature near 327 MHz, and computing the total column length for the radiation by assuming a Galactic disk of radius 15 kpc (see eq. [4]). The equivalent temperature of background radiation within the cloud (see eq. [5]) is computed for each model cloud size S using the assumed total column length for the radiation and the measured continuum temperature near 327 MHz. The radiation temperature is scaled to different frequencies using a spectral index of −2.7 (Salter & Brown 1988).

3.4. *Density of the Line Emitting Cloud*

One important aspect of the interpretation of the low-frequency RRL emission is that the density of the ionized gas is well constrained just from the recombination line observations near 1.4 GHz and 327 MHz (Anantharamaiah

1985b, also see below). This is because of the markedly different dependence of line intensity on density at the two frequencies. We have used this aspect for estimating the density of the ionized gas at various observed positions. The angular resolution ($\sim 2^\circ \times 2^\circ$) of 327 MHz observations (Paper I) is coarse compared to that of the observations near 1.4 GHz. The HPBW of the observations by Lockman (1976, 1980) was 21′, those by Hart & Pedlar (1976b) were 31′ × 33′, those by Cersosimo (1990) were 34′, and those by Heiles et al. (1996b) were 36′ (also 21′ for the observations with the 140 foot [43 m] telescope). All together there were about 274 positions observed near 1.4 GHz in the longitude range of interest (i.e., 332° to 0° to 89°) and within $b = \pm 1^\circ$. To obtain the line intensity near 1.4 GHz that would be observed with a beam similar to that of 327 MHz observations, we followed the scheme described below. Care was taken to eliminate those positions observed at 1.4 GHz which had possible contribution from known, small-diameter H II regions since such objects would not have contributed to the observed line emission at 327 MHz. H II regions were identified using the continuum maps of Altenhoff et al. (1979) and Reich et al. (1990) and higher frequency RRL observations of Caswell & Haynes (1987), Lockman (1989), and Lockman, Pisano, & Howards (1996). Using these criteria, a total of 137 positions observed in RRLs at 1.4 GHz were selected. Using these data, composite spectra were constructed from Gaussian components of the lines detected in all the observed spectra inside the $\sim 2^\circ \times 2^\circ$ beam. Examples of composite spectra are shown in Figure 1. The line parameters were then obtained from a single-component Gaussian fit to these composite spectra. If a composite spectrum contained spectral components with "large" difference in central velocities, then the parameters of the component with the central velocity nearest to that of the line detected at 327 MHz were obtained with a single-component Gaussian fit. Most of the positions ($\sim 92\%$) had only one component in the composite 1.4 GHz spectrum and the central velocity of the spectral feature matched within ± 5 km s^{-1} of the line observed near 327 MHz. The width of the line in some cases, however, was larger than that observed near 327 MHz. The peak line temperature obtained from the composite spectra was taken as the line brightness temperature near 1.4 GHz and is given in Table 1.

Table 1 gives the input parameters used for modeling. The method used for constraining the density of the ionized gas is illustrated using the data at the position G11.6+0.0. The modeling starts with the computation of the departure coefficients, which are functions of the electron density and temperature. We used the computer code originally developed by Brocklehurst & Salem (1977) and later modified by Walmsley & Watson (1982) and Payne, Anantharamaiah, & Erickson (1994) for the computation of the departure coefficients. Two of the input parameters for this computation, namely, the nonthermal background temperature at 100 MHz, T_{R100}, and its spectral index α were assumed to be 10,000 K and -2.7, respectively, which are mean values for the Galactic plane (Haslam et al. 1982; Salter & Brown 1988). The departure coefficients for the model parameters are obtained by interpolating from a precomputed table on a grid of electron temperatures and densities. The emission measure that is required to produce the observed line inten-

TABLE 1

LINE AND CONTINUUM PARAMETERS FOR MODELING

l ($b=0^\circ$) (deg.)	T_L 1.4 GHz (mK)	T_L 327 MHz (mK)	ΔV 327 MHz (km s^{-1})	V_{LSR} 327 MHz (km s^{-1})	T_C[a] 327 MHz (K)	T_C[a] 2.7 GHz (K)	T_C[a] 10 GHz (K)
332.1.....	43	133	47.8	−58.4	257	...	...
340.3.....	50	120	54.1	−36.3	313	...	...
357.6.....	23	291	26.2	−1.2	714	...	...
0.0	102	664	29.0	5.9	1085	7.2	0.47
2.3	13	209	26.0	10.2	699	3.7	0.10
4.7	26	378	28.8	11.3	644	3.5	0.07
7.0	29	347	24.8	20.6	685	4.1	0.14
9.3	24	255	33.9	19.6	624	3.6	0.11
11.6	35	269	43.0	27.2	591	3.4	0.10
13.9	27	513	38.1	26.9	657	4.1	0.19
16.1	46	375	46.6	28.8	568	4.0	0.14
18.4	31	298	30.6	30.0	599	3.4	0.13
20.7	17	142	34.2	55.2	540	3.0	0.11
36.5	21	107	60.0	65.2	407	2.3	0.08
41.0	13	59	36.3	55.1	348	1.8	0.05
45.5	12	60	40.5	48.8	267	1.4	0.04
50.0	14	52	58.3	50.5	268	2.1	0.12
54.6	9	41	14.2	31.4	150	1.0	...
59.2	11	39	21.0	25.2	109	0.8	...
61.5	10	38	34.9	29.4	104	0.8	...
63.8	13	38	14.7	22.6	88	0.7	...
73.3	9	30	29.1	22.6	86	1.0	...
75.8	12	44	39.9	3.4	105	...	...
78.2	45	125	35.1	3.1	183	...	...
80.7	64	142	28.5	4.1	185	...	...
83.3	58	75	37.8	3.8	113	...	...

[a] Continuum temperatures at 327 MHz, 2.7 GHz, and 10 GHz.

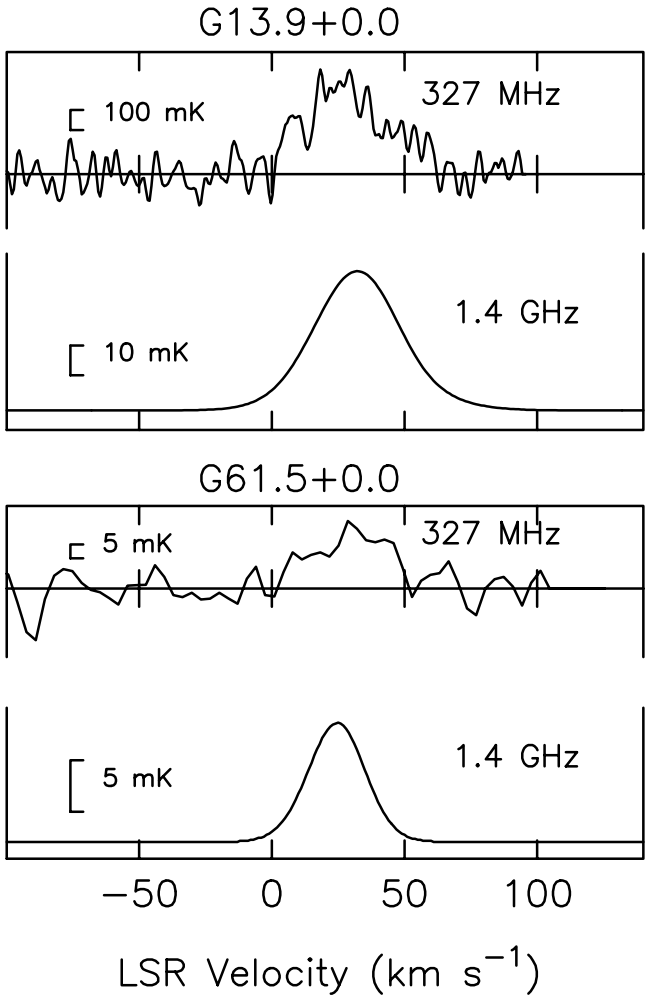

FIG. 1.—Composite spectra toward the positions G13.9+0.0 and G61.5+0.0 obtained from 1.4 GHz RRL data taken from Lockman (1976, 1980), Hart & Pedlar (1976b), and Heiles et al. (1996b; *bottom frame*) along with 327 MHz spectra taken from Paper I (*top frames*) toward the same positions. The 327 MHz spectra are from observations with a beam of $2^\circ \times 2^\circ$ (Paper I). The 1.4 GHz spectra are constructed by adding the Gaussian components of the lines detected in all the available spectra in the same region. The amplitude scale for each of the spectrum is marked separately.

sity is then obtained iteratively using equation (1). For a given combination of electron density and temperature, the expected line width caused by both Doppler and pressure broadening were taken into account. The background radiation temperature *at the cloud position* is obtained as discussed in § 3.1. Figure 2*a* shows a plot of the estimated emission measure as a function of density for various temperatures. At each electron temperature, the intersection points of the curves corresponding to RRLs at 1.4 GHz and 327 MHz give the density of the gas. The electron density is well determined within a factor of 2 regardless of the temperature and emission measure. The uncertainties in the estimated density are caused mainly by (1) the uncertainty in the estimated angular size, (2) the assumption that the Galactic background radiation has a uniform emissivity, and (3) uncertainty in the estimated distance.

The density of the ionized gas estimated for different positions using the method described above is given in Table 2. The derived densities are in the range of 1–10 cm^{-3}. Figure 3 shows a histogram of the derived electron densities. These values are consistent with the earlier estimates of density of the ionized gas by Anantharamaiah (1985b, 1986).

3.5. *Constraining the Temperature and the Size of the Ionized Region*

It is not possible to obtain an unique combination of the temperature and the size of the line emitting region just from the 327 MHz and 1.4 GHz data (Anantharamaiah 1985b). This impossibility is illustrated in Figure 2*b* for the data at position G11.6+0.0. In this figure, using the density as determined above, the emission measures required for producing the measured RRL intensity near 1.4 GHz and 327 MHz are plotted as a function of electron temperature. A large range of emission measures and a correspondingly large range of temperatures can produce the observed line intensity at the two frequencies. Figure 2*b* also shows that no further constraints are imposed by the upper limit for the line to continuum ratio at 75 MHz of $\sim 10^{-4}$ observed by Erickson et al. (1995). The parameter space to the right of the 75 MHz curve is consistent with the upper limit and thus could provide only a cross check on the consistency of the model obtained from the 1.4 GHz and 327 MHz lines. For the position G13.9+0.0, no solution consistent with the 75 MHz upper limit could be obtained.

In directions where the model is consistent with all the RRL observations, upper limits on the electron temperature and the size of the line emitting region were estimated using other criteria. These criteria are (1) the line width, (2) continuum emission from the ionized region, and (3) the dispersion measure (DM) produced by the region. The line width caused by Doppler broadening cannot exceed the observed line width if we assume that the broadening is purely because of thermal motions, thus providing an upper limit to the temperature. This upper limit is significant only for the positions where narrow (<15 km s^{-1}) lines were observed. The ionized gas responsible for RRL emission also produces continuum emission, the intensity of which is a function of electron temperature and emission measure (Shaver 1975). The measured continuum at the observed positions have contribution from both thermal emission from the cloud and nonthermal emission from the Galactic background. At frequencies higher than a few GHz, a good fraction of the continuum emission ($\sim 50\%$ at 10 GHz in the inner Galaxy; Broadbent, Osborne, & Haslam 1989) is thermal; hence, the measured continuum temperature at these frequencies can be used as a further constraint. The measured continuum temperature can have contribution from the nonthermal background emission as well as from other ionized components that are not detected in RRLs near 327 MHz and thus can only provide an upper limit to emission from the ionized gas producing the observed RRLs. The continuum temperature toward the observed positions near 2.7 and 10 GHz were obtained from the maps of Reich et al. (1990) and Handa et al. (1987), respectively. To get an average continuum temperature toward the observed positions, both these maps were convolved with a beam comparable to the resolution of the 327 MHz RRL survey. The continuum temperatures thus obtained for these frequencies are given in Table 1. For the data at the position G11.6+0.0, the cloud parameters that can produce the observed continuum temperatures are indicated by two curves marked appropriately in Figure 2*b*. The intersection of these curves with those obtained from RRL

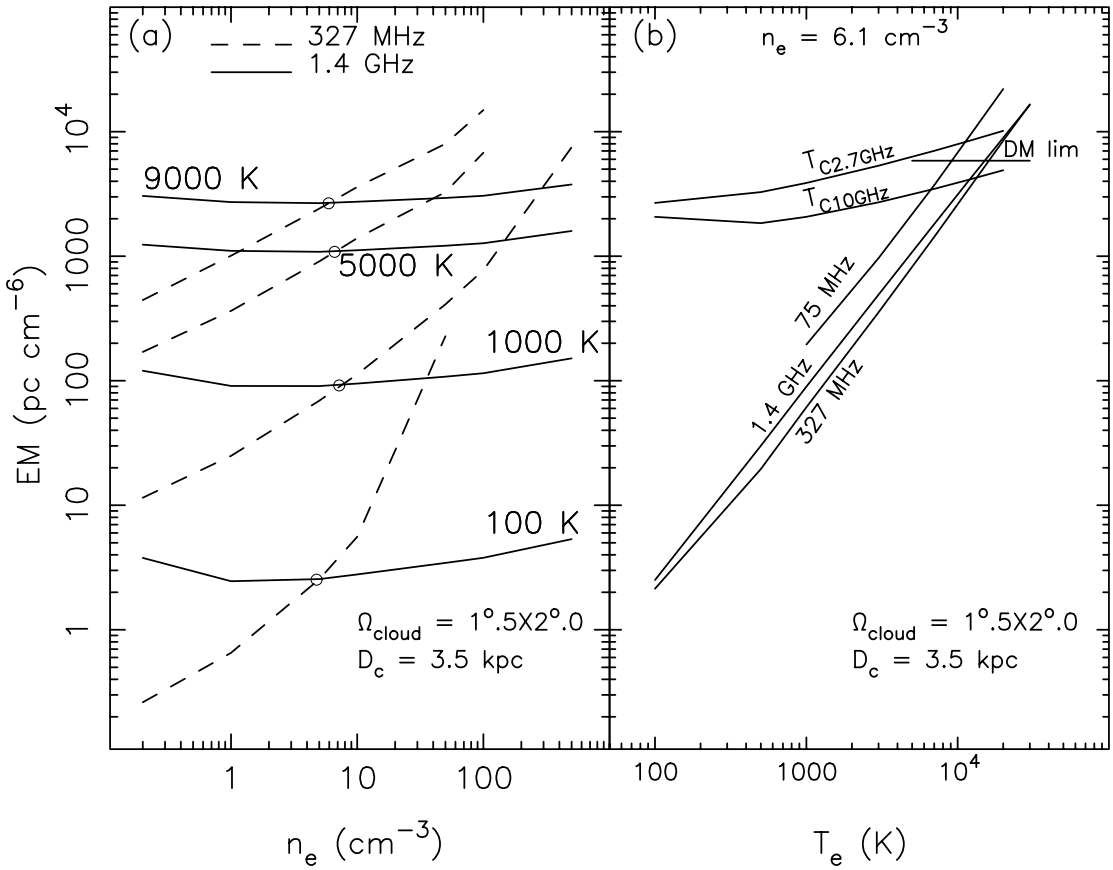

FIG. 2.—Constraints on the physical properties of the gas producing RRL emission near 327 MHz toward the direction $l = 11\overset{\circ}{.}6$ and $b = 0\overset{\circ}{.}0$. The kinematic distance to the cloud and the assumed angular size are indicated at the bottom right. (*a*) Plot of the emission measure required to produce the observed line intensity as a function of electron density at four different temperatures as marked. The dashed lines are for line emission near 327 MHz and the solid lines are for the 1.4 GHz line emission. The density of the gas, defined by the intersection point of the two curves (marked by open circles), is well constrained at about 6.1 cm^{-3} for any temperature. (*b*) Plot of the emission measure required to produce the observed line and continuum intensity as a function of electron temperature. The density as determined from (*a*) is used to obtain this plot. The curves marked 327 MHz and 1.4 GHz are the set of parameters consistent with RRL observations at these frequencies. The parameter space consistent with the upper limit obtained on RRL emission at 75 MHz is to the right side of the curve marked 75 MHz. The plot of emission measure required to produce the observed continuum brightness temperatures at 2.7 and 10 GHz for different electron temperature are marked $T_{C2.7\ GHz}$ and $T_{C10\ GHz}$, respectively. The intersection of the curve "DM lim" with those marked 327 MHz and 1.4 GHz gives an upper limit on the emission measure, and thus on the temperature, from consideration of dispersion measure, obtained from the electron density model of Taylor & Cordes (1993).

observations gives an upper limit to the temperature and thus an upper limit to the size of the line emitting region.

Study of the dispersion of pulsar signals gives the column density of electrons along the line of sight. Analysis of DM measured toward pulsars of known distances was used by Taylor & Cordes (1993) to construct a free-electron density model of the Galaxy. We impose the constraint that the DM caused by the ionized gas that produces the observed RRLs should be less than that obtained from the electron density model of Taylor & Cordes (1993). The DM in a given direction is obtained from the electron density model by considering a Galactic disk of radius 15 kpc and integrating the electron density over the line of sight to the edge of the disk. The upper limits on the electron temperature and size obtained toward G11.6+0.0 using this criteria are shown in Figure 2*b*. The DM estimated from the electron density model in this direction is $\sim$1400 pc cm^{-3}.

The range of physical parameters for the ionized regions obtained using the above criteria is large. This large range is clear from Figure 2*b* for the case of G11.6+0.0. The derived upper limits on the electron temperature and the size for all the directions and the criterion that resulted in the upper limits are given in Table 2. The upper limit for the temperature is typically 12,000 K and that for the path length is $\sim$500 pc. For a few positions, the temperature of the line emitting region is constrained by the observed line width. The upper limits thus obtained are, in some cases, less than 5000 K. These regions may be similar to the low-temperature H II regions reported earlier by Shaver, McGee, & Pottasch (1979) and Lockman and colleagues (1989, 1996). Since the temperature is not well constrained for other positions, we estimated the path length through the line emitting region by assuming $T_e = 7000$ K for the ionized gas, which is close to the mean temperature of H II regions near the solar circle as determined by Shaver et al. (1983). This temperature is also consistent with the value obtained by Heiles et al. (1996b) for the low-density ionized gas from RRL observations near 1.4 GHz. The estimated path lengths are in the range of 20–200 pc (see Table 2). Figure 4 shows the histogram of the estimated path lengths. These values are comparable to those estimated by Anantharamaiah (1985b).

For most of the positions, the derived parameters corresponding to both "near" and "far" kinematic distances are

TABLE 2

DERIVED PHYSICAL PROPERTIES

l[a] (deg.)	$\Omega_{cloud}\eta_B/\Omega_B$[b]	D_c (kpc)	n_e (cm^{-3})	S[c] (pc)	Upper Limit T_e (K)	Upper Limit S (pc)	Note
332.1.....	0.15	4.1	3.0	310	8800	430	a
		10.9	1.9	...	6400	660	a
340.3.....	0.19	3.1	9.9	35	18300	145	a
		12.9	5.4	120	12100	270	a
357.6.....	0.33	4.2	2.4	120	14800	460	b
0.0	0.34	4.2	11.3	25	17400	110	a
2.3	0.34	4.2	1.8	130	14600	490	b
4.7	0.35	3.1	2.1	200	13400	590	a
7.0	0.35	3.9	2.8	100	13300	320	b
9.3	0.36	3.0	3.7	70	18500	370	a, c
11.6	0.36	3.5	6.1	50	11700	110	c
		13.2	3.1	200	11100	400	a, c
16.1	0.37	2.8	6.1	70	11600	150	c
		13.5	2.9	340	9100	500	a
18.4	0.38	2.7	4.4	60	18900	310	c
		13.4	2.1	300	12300	730	a
20.7	0.38	4.4	4.5	35	23000	260	a, c
		11.5	2.9	95	19600	520	a
36.5	0.38	4.5	9.4	20	10300	30	c
		9.2	7.1	35	10100	60	c
41.0	0.38	3.7	8.3	10	15600	35	c
		9.1	6.1	20	15200	60	c
45.5	0.38	3.3	5.4	20	13200	60	c
		8.6	3.6	50	13200	140	c
50.0	0.37	4.0	11.2	10	19400	45	a, c
		6.9	8.8	15	16900	60	a
54.6	0.36	2.3	3.3	...	4400	10	b
		7.5	2.3	...	4400	20	b
59.2	0.35	2.0	3.6	30	9500	45	b
		6.7	2.7	50	9500	80	b
61.5	0.35	2.9	3.1	60	12200	135	a
		5.2	2.6	80	11000	160	a
63.8	0.34	2.1	3.7	...	4700	10	b
		5.4	2.9	...	4700	20	b
73.3	0.26	1.2	1.7	130	9600	220	a
		3.6	1.5	180	8700	250	a
75.8	0.25	4.0	1.5	...	5900	245	a
78.2	0.23	3.3	5.0	...	6200	70	a
80.7	0.22	2.6	7.3	45	7150	50	a
83.3	0.21	1.9	16.3	10	10500	20	a

NOTE.—Two entries given for some of the positions correspond to "near" and "far" kinematic distances D_c. The last column indicates the criterion that resulted in the upper limit: "a" equals limit from DM; "b" equals limit from line width; "c" equals limit from 10 GHz continuum.

[a] $b = 0°$ for all positions.

[b] Factor used to convert the observed line antenna temperature near 327 MHz to line brightness temperature.

[c] Estimated path length for an assumed electron temperature T_e of 7000 K for the ionized gas.

given in Table 2. In the longitude range $l = 75°$ to 83°, the Hα intensity obtained from the models with "near" distance, after taking into account interstellar extinction, are not consistent with that observed by Reynolds (1983). Therefore, for these positions, the parameters were estimated assuming the "far" distance.

In the longitude range $l = 5°$ to 10°, no model consistent with the 75 MHz upper limit could be obtained when the ionized gas is placed at the "far" distance.

4. COMPARISON WITH OTHER RELATED OBSERVATIONS

Widespread presence of low-density ionized gas in the inner Galaxy is evident from other observations as well. Examples are (1) free-free absorption of the Galactic non-thermal background radiation in the inner Galaxy at frequencies less than 100 MHz (Westerhout 1958; Shain, Komesaroff, & Higgins 1961; Broadbent et al. 1989; Dwarakanath 1989) and (2) presence of widespread emission of diffuse [N II] 205 μm and [C II] 158 μm fine-structure transitions in the Glactic plane (Wright et al. 1991; Nakagawa et al. 1998). This section uses the derived electron density and the estimated path lengths of RRL emitting gas for an assumed temperature of 7000 K (wherever upper limits on T_e exceed 7000 K) to estimate the expected intensities of [N II] 205 μm, [C II] 158 μm, and Hα lines from this ionized component. The absorption of the Galactic background emission near 34.5 MHz caused by this low-density ionized gas is also estimated using these

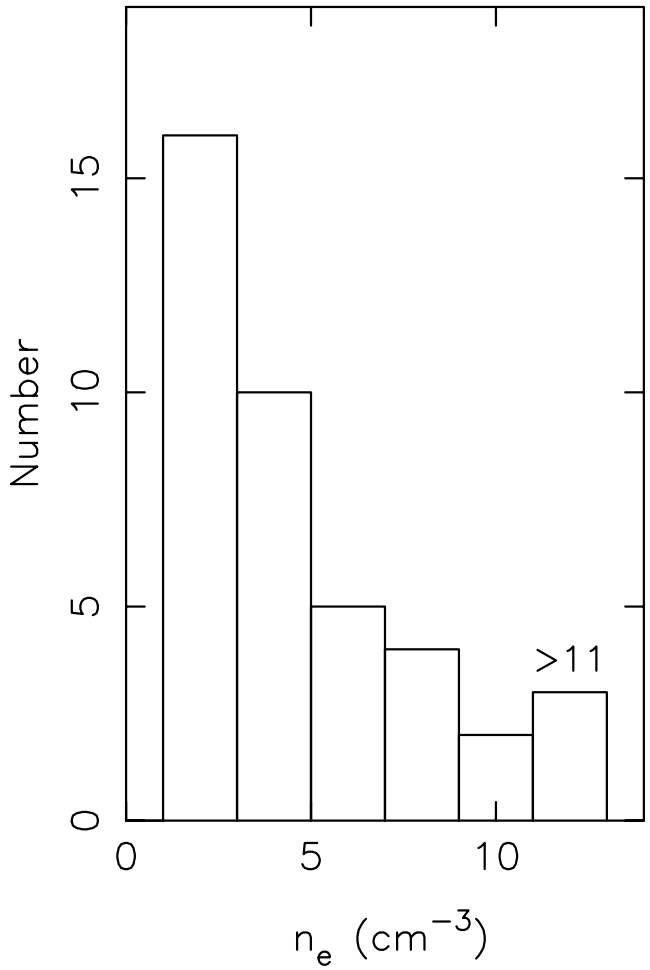

FIG. 3.—Histogram of the derived electron densities of the ionized gas producing the RRL emission near 327 MHz. The estimated densities for both "far" and "near" distances are used to obtain this histogram.

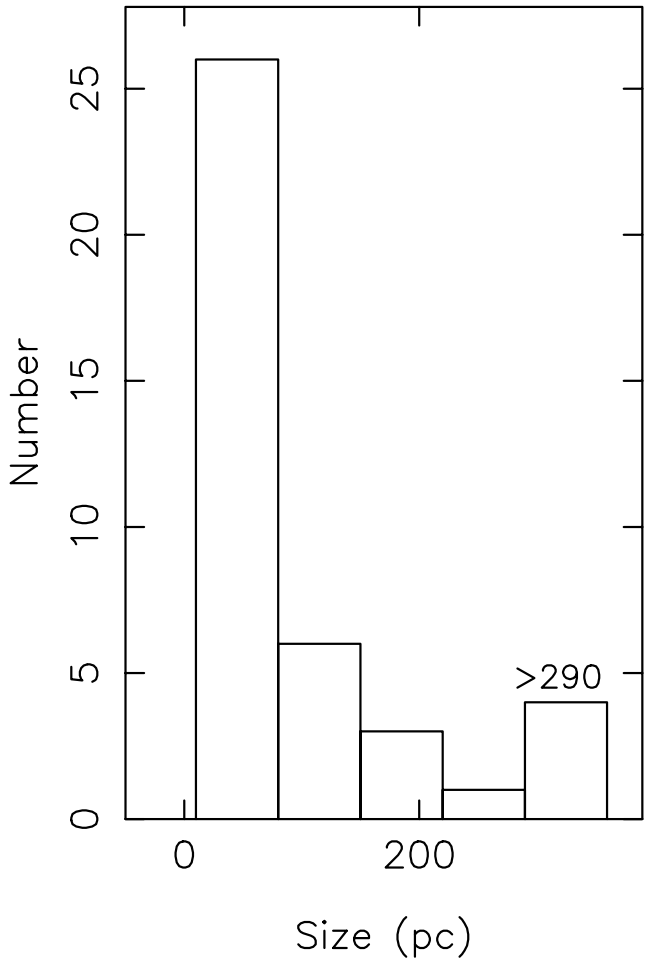

FIG. 4.—Histogram of the estimated path lengths of the ionized gas producing the RRL emission near 327 MHz. To estimate the path lengths, the temperature of the ionized gas is assumed to be 7000 K. The upper limits on the path lengths for positions where the maximum allowable temperature is less than 7000 K are also included in the histogram. Also, the estimated path lengths for both "far" and "near" distances are included in the histogram.

parameters. The estimated values are compared with the observations.

4.1. *Absorption of Galactic Background Emission at 34.5 MHz*

Our aim is to estimate the effect of the low-density ionized gas on the nonthermal background radiation near 34.5 MHz and compare it with the observed brightness temperature. The expected brightness temperature near 34.5 MHz in the absence of such ionized clouds can be estimated approximately using the measured brightness temperature at 408 MHz (Haslam et al. 1982) and scaling it to 34.5 MHz using the relation $T_B \propto \nu^{\alpha}$ with the spectral index $\alpha = -2.7$ (Salter & Brown 1988). Any ionized cloud along the line of sight attenuates the background radiation by a factor $e^{-\tau_c}$, where τ_c is the free-free optical depth. The net observed radiation intensity also has an unattenuated contribution from the foreground, which we compute using a simple model where the ionized region is placed at a distance D_c from Sun. The background and foreground nonthermal emission are assumed to have a uniform emissivity in the Galactic disk. We assume that the ionized region is homogeneous and has an angular size of 1°.5 (along b) × 2° (along l). The total column length $D_{\rm bg}$ in a given direction is obtained by assuming a Galactic disk of radius 15 kpc. Using the solution of the radiative transfer equation, the observed brightness temperature T_o can then be written as

$$T_o(\nu) = \frac{T_{\rm sky}(\nu)}{D_{\rm bg}}\,(D_{\rm bg} - D_c)e^{-\tau_c} + T_e(1 - e^{-\tau_c}) + \frac{T_{\rm sky}(\nu)}{D_{\rm bg}}\,D_c\,, \tag{7}$$

where $T_{\rm sky}(\nu)$ is the observed background brightness temperature in the absence of the cloud. $[T_{\rm sky}(\nu)/D_{\rm bg}](D_{\rm bg} - D_c)$ and $[T_{\rm sky}(\nu)/D_{\rm bg}]D_c$ are the contribution to the net brightness temperature from behind and in front of the cloud, respectively.

The result of the computation is shown in Figure 5. For comparison with observations, the brightness temperature near 34.5 MHz is obtained from the continuum map of Dwarakanath & Udaya Shankar (1990). The brightness temperature near 34.5 MHz and the temperature scaled from 408 MHz observations are obtained after convolving the respective continuum maps to an angular resolution of 1°.5 × 1°.5. Figure 5 shows that the absorption of the background radiation caused by the low-density ionized gas is

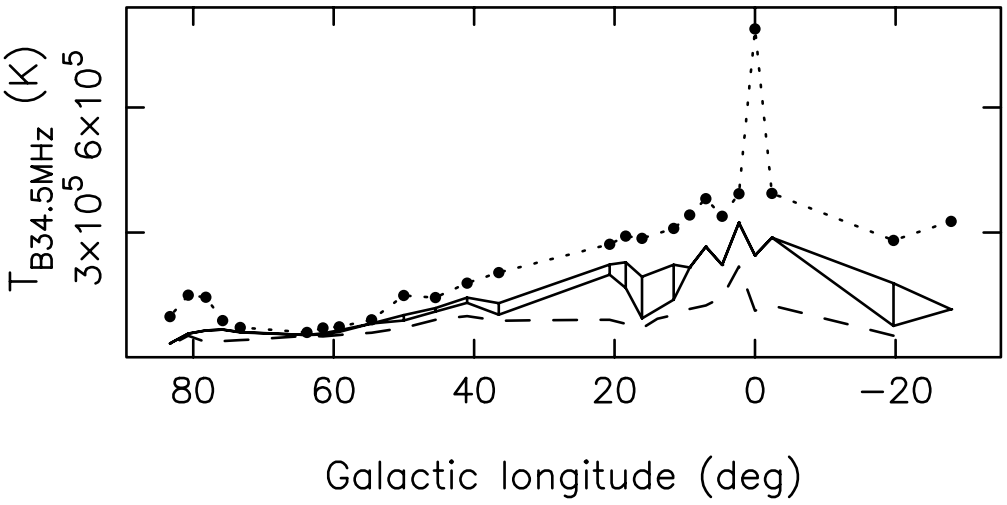

FIG. 5.—Free-free absorbing effects of the RRL producing ionized regions on the continuum brightness temperature along the Galactic plane at 34.5 MHz. The expected continuum temperature at 34.5 MHz without any absorption scaled from 408 MHz values taken from Haslam et al. (1982) and using a spectral index of −2.7 is shown as a dotted line. The solid line represents the estimated brightness temperature at 34.5 MHz after taking into account the absorption by RRL-producing gas. The dots indicate the positions at which estimates were made. Estimates made for both "near" and "far" kinematic distance are plotted as solid lines. The observed continuum at 34.5 MHz, taken from Dwarakanath & Udaya Shankar (1990), is shown as a dashed line.

significant; it accounts for ~50% of all the observed absorption. This computation takes into account only the low-density ionized gas that is responsible for RRL emission near 327 MHz along each line of sight. In reality, there are other forms of ionized gas present in the Galactic disk that can contribute to the continuum absorption at low frequencies. For example, the ionized gas responsible for optical nebulosities cataloged by Rodgers, Campbell, & Whiteoak (1960) and Sivan (1974) can add to the continuum absorption (Dwarakanath 1989). The limitations of the above calculations are (1) the background temperature at the cloud position is estimated by assuming a uniform emissivity for the Galactic nonthermal radiation, (2) uncertainty in the physical properties of the low density ionized gas (see Table 2), and (3) uncertainty in the estimated distances to the ionized gas.

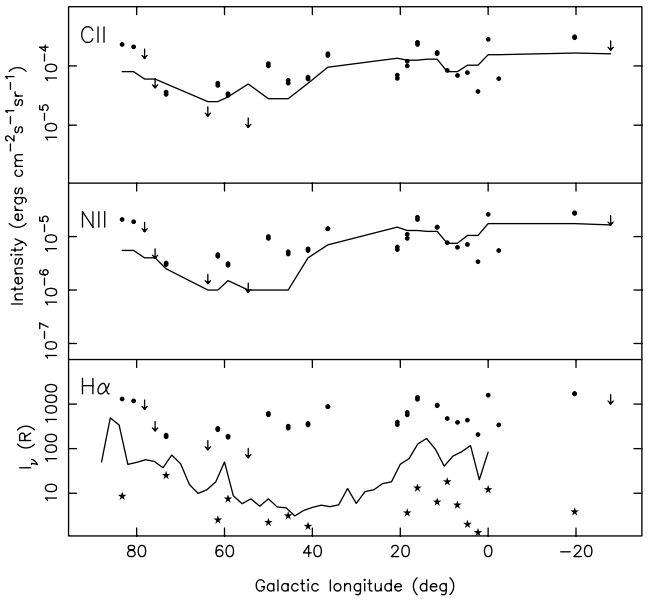

FIG. 6.—Estimated far-infrared fine-structure line emissions ([C II] 158 μm and [N II] 205 μm) and Hα emission from the RRL-producing gas in the inner Galaxy. The computed values are marked by dots and the arrows represent upper limits. The expected Hα intensity after applying an estimated interstellar extinction are shown as stars. The solid line is the measured line emission at different positions. The [C II] and [N II] line intensities are from the *COBE*-FIRAS measurements (Wright et al. 1991), which are an average over a beam of 7° × 5°. The Hα measurements are taken from Reynolds (1983).

4.2. [C II], [N II], *and Hα Emission*

For a temperature of 7000 K, the critical density below which [C II] 158 μm and [N II] 205 μm transitions can occur are ~30 cm^{-3} and ~150 cm^{-3}, respectively (Osterbrock 1989). The derived densities of the ionized gas responsible for the RRL emission are much smaller than these critical densities. We therefore explore the possibility that the fine-structure lines are produced in the same ionized region that are responsible for RRL emission near 327 MHz.

The equations used for the computation of the fine-structure line intensities are (Heiles 1994)

$$I_{[\mathrm{C\ II}]} = 1.55 \times 10^{-7} \delta_{C^+} T_e^{-0.35} n_e^2 S\,, \quad (8)$$

$$I_{[\mathrm{N\ II}]} = 1.55 \times 10^{-9} \delta_{N^+} T_e^{-0.5} n_e^2 S\,, \quad (9)$$

where the $I_{[\mathrm{CII}]}$ and $I_{[\mathrm{NII}]}$ are the intensities (ergs cm^{-2} s^{-1} sr^{-1}) of [C II] 158 μm and [N II] 205 μm transitions, respectively; δ_{C^+} and δ_{N^+} account for depletion onto dust grains or other ionization states of C and N, respectively; T_e is in units of 10^4 K; n_e and S are in units of cm^{-3} and pc, respectively. These equations are good approximations for temperatures in the range 4000–10,000 K and densities much less than the critical density. Cosmic abundances of C/H = 4×10^{-4} and N/H = 1×10^{-4} are assumed for obtaining the equations. We have used depletion factors of 0.5 for C and 0.78 for N for the computation of line intensities (Heiles 1994). The estimated line intensities of the fine-structure transitions of [C II] and [N II] as a function of Galactic longitude using the physical properties of the ionized gas given in Table 2 are shown in Figure 6. The

intensities of these lines measured with the *COBE*'s Far Infrared Absolute Spectrophotometer (FIRAS; Wright et al. 1991) are also plotted (*solid line*) in the figure. The *COBE*-FIRAS measurements were averaged over a beam of $7^\circ \times 5^\circ$. Thus it is not possible to do a quantitative study at this stage. The estimated intensities are comparable to the *COBE*-FIRAS measurements indicating that most of [N II] and [C II] emissions could originate in the low-density ionized gas that is responsible for the RRL emission observed near 327 MHz.

Accurate LSR velocity measurements of the fine-structure lines are not yet available for all the directions in the inner Galaxy. Results of balloon-borne observations of [C II] 158 μm transitions from the Galactic plane in the longitude range -10° to 25° are presented by Nakagawa et al. (1998). The angular resolution of these observations are $15'$. The *l-v* diagram obtained from this data shows a good similarity with that obtained from the RRL observations in the Galactic plane. Thus, we conclude that a considerable amount of the observed [C II] lines originate in the low-density ionized gas that is responsible for the RRL emission at 327 MHz and 1.4 GHz. This conclusion is consistent with the suggestion by Heiles (1994).

The Hα intensities from the RRL emitting low-density ionized gas are computed using the equation (Heiles 1994)

$$I_{\mathrm{H}\alpha} = 0.36 T_e^{-0.9} n_e^2 S \, , \qquad (10)$$

where $I_{\mathrm{H}\alpha}$ is the intensity of Hα emission in Rayleigh ($= 2.4 \times 10^{-7}$ ergs cm^{-2} s^{-1} sr^{-1}), T_e is in units of 10^4 K, n_e and S are in units of cm^{-3} and pc, respectively. The observable intensity of Hα emission, however, will be less than the computed values because of interstellar extinction. We have used values of A_v obtained from the visual extinction model of Hakkila et al. (1997) to take account of this attenuation. Figure 6 (*bottom frame*) shows the estimated Hα intensity, computed using equation (10), along with observed values taken from Reynolds (1983). The Hα intensity obtained after applying the attenuation caused by interstellar extinction is also shown in Figure 6. Figure 6 shows that most of the Hα emission from the ionized gas producing RRL emission near 327 MHz is not observed in the Hα survey of Reynolds (1983) because of large interstellar extinction.

The lines detected in the Hα survey consist of emission from discrete regions apart from a fainter, smoothly varying Hα background (Reynolds 1983). The smooth background emission originates from ionized gas with an rms electron density of ~ 0.1 cm^{-3} and is extended within ~ 1 kpc from the Sun. The 327 MHz RRL survey is not sensitive enough to detect radio recombination lines from this gas. RRLs from discrete ionized regions producing Hα emission are detectable in some cases (Reynolds 1983). However, in most of the directions, either the lack of sensitivity of the RRL observations or the interstellar extinction of Hα radiation make it difficult to detect both Hα and radio lines from the same ionized gas. Thus, low-frequency RRL observations complement the Hα survey.

5. ORIGIN OF THE LOW-DENSITY IONIZED GAS IN THE GALAXY

5.1. *Results from the 327 MHz RRL Survey*

The basic results from Papers I and II and the analysis presented in § 3 of this paper can be summarized as follows.

1. In the low-resolution ($2^\circ \times 2^\circ$) survey, hydrogen RRLs were detected in almost all positions in the longitude range $l = 330^\circ$ to 0° to 89° (Paper I).

2. In the outer Galaxy ($l = 172^\circ$ to 252°), hydrogen lines were marginally detected in only three positions of the 14 observed. These observations were also made with an angular resolution of $2^\circ \times 2^\circ$ (Paper I).

3. Along the Galactic latitude, lines were detected up to $b = \pm 3^\circ$ in the low-resolution survey. A lower limit to the scale height of line emission of ~ 100 pc was deduced from these observations (Paper I).

4. In the inner Galaxy, the velocity-integrated line intensity shows large fluctuations as a function of Galactic longitude. These fluctuations imply that the line emitting region is not a uniform homogeneous medium (Paper I).

5. The line emission is well correlated (correlation coefficient = 0.88) with the nonthermal continuum emission in the same direction indicating that stimulated emission is dominant (Paper I).

6. The *l-v* diagram and the derived radial distribution of RRL emission at 327 MHz show good agreement with those of "intense" ^{12}CO emission and to some extent with those of high-frequency RRL emission from H II regions. On the other hand, the distribution of the Hα emission and H I emission in the Galactic disk is different from that of the RRL emission near 327 MHz (Paper I).

7. Higher resolution ($2^\circ \times 6'$) observations were made toward a selected set of $2^\circ \times 2^\circ$ fields that were observed in the low-resolution survey. For $l < 35^\circ$, hydrogen RRLs were detected in almost all the positions within the $2^\circ \times 2^\circ$ field. The line emission, however, does not appear to originate from a homogeneous medium and in many cases shows structures over an angular scale of $\sim 6'$. For $l > 35^\circ$, a comparatively fewer number of lines were observed within the $2^\circ \times 2^\circ$ field (Paper II).

8. Analysis of line emission observed in the higher resolution survey toward the $2^\circ \times 2^\circ$ field centered at $l = 45.^\circ 5$, $b = 0^\circ$ indicates that an individual line emitting region may have an angular size $\geq 1^\circ$. This angular size corresponds to a linear size greater than 110 pc for a kinematic distance of ~ 6.3 kpc. The central velocities of the line emission at different positions within the 2° wide field are comparable with those of the H II regions in the field (Paper II).

9. The median width of the hydrogen lines observed in both high- and low-resolution surveys is ~ 30 km s^{-1}, which is somewhat larger than the median line width observed from normal H II regions (~ 26 km s^{-1}; Papers I & II).

10. The density of the ionized gas as derived by combining the 327 MHz data with the RRL observations near 1.4 GHz is in the range 1–10 cm^{-3}. Upper limits obtained for the temperature and size of the line emitting regions are $\sim 12{,}000$ K and ~ 500 pc, respectively. The sizes of the line emitting regions estimated by assuming a temperature of 7000 K for the ionized gas are in the range 20–200 pc (§ 3).

The origin of low-density ionized gas responsible for low-frequency RRL emission in the Galaxy is not well understood although several observations exist. Some of the suggestions based on earlier work are that the lines originate (1) in an extended low-density warm ionized medium (ELDWIM) proposed by Petuchowski & Bennett (1993) (Mezger 1978; Heiles 1994; Heiles et al. 1996b), (2) in low-density envelopes of compact, high-density H II regions

(Hart & Pedlar 1976a; Lockman 1980; Anantharamaiah 1986), and (3) in evolved H II regions (Matthews et al. 1973; Shaver 1976). The following subsections reexamine these models in the light of our new observations and results.

5.2. *Extended Low-density Warm Ionized Medium (ELDWIM)*

Mezger (1978) suggested that the low-frequency RRL and diffuse free-free radio continuum emission in the inner Galaxy originate from extended low-density gas. He portrayed this gas as an ensemble of Galactic extended low-density (ELD) H II regions; the size of these ELD H II regions are large enough for their Strömgren spheres to partially overlap. This picture was further developed by Petuchowski & Bennett (1993). They suggested a morphological model in which the extended low-density ionized gas is conflated with the well-known WIM and referred to it as the "extended low-density warm ionized medium" (ELDWIM). In their definition of ELDWIM, Petuchowski & Bennett (1993) consider all ionized gases with density less than 40 cm^{-3} (about a factor of 3 less than the critical density of [N II] 205 μm transition) as one medium. In the interpretation of their 1.4 GHz RRL survey, Heiles et al. (1996a, 1996b) referred to the ionized gas responsible for "diffuse RRL emission near 1.4 GHz" as ELDWIM. For the present discussion, we consider ELDWIM as a medium semipervasive in the inner Galaxy and having extended morphology as discussed by Petuchowski & Bennett (1993) and Heiles (1994) and is further elaborated below.

In the ELDWIM model (Petuchowski & Bennett 1993; Heiles 1994), the ELD H II regions responsible for RRL emission are produced by bare O stars that are formed in the late stage of evolution of H II regions (Mezger 1978). It is believed that all O stars are formed in dense clouds of gas, which, when ionized, produce an associated radio H II region. The O stars outlive the radio H II region phase because of their longer lifetime (6×10^6 yr) compared to that of the H II regions (lifetime $\sim 5 \times 10^5$ yr; Smith, Biermann, & Mezger 1978), thus forming bare O stars. The RRL observations, however, show that the line emission is associated with currently active star-forming regions. This association is evident from the fact that the distribution of RRL emission near 327 MHz in the Galactic disk is similar to that of "intense" ^{12}CO emission and compact, higher density H II regions (Paper I). The "intense" ^{12}CO emission originate from the "warm" molecular clouds, which are sites of active star formation (Solomon, Sanders, & Rivolo 1985). Since ELDWIM is pictured as a semipervasive medium, not necessarily associated with star-forming regions (Petuchowski & Bennett 1993), the above argument suggests that ELDWIM is not a favored site for the origin of low-frequency RRLs. One caveat to the above argument is that the angular resolution of the 327 MHz observations is 2°; hence, the linear scale sampled by the beam at a typical distance of 5 kpc is $\sim$200 pc, which is much greater than the typical size of giant molecular clouds ($\sim$40 pc; Combes 1991).

A distinguishing characteristic of the ELDWIM model is that the low-density ionized gas is pervasive and widely distributed in the inner Galaxy (Heiles 1994). This implies that the filling factor of this medium should be large, at least in the inner Galaxy. Our estimates of the physical properties in § 3, however, indicate that the low-density gas producing RRLs has a path length of only 20–200 pc for a typical temperature of 7000 K for the ionized region. If we consider the radius of the Galactic disk to be 15 kpc, then the filling factor of this ionized gas is less than 1%. This value is comparable with that derived by Heiles et al. (1996b) toward the direction $l \sim 20°$ in the Galactic plane. The filling factors cannot be, in any case, higher than 3% since the upper limit on the path lengths obtained from our analysis is $\sim$500 pc. Furthermore, the low-frequency RRLs have a median line width $\sim$30 km s^{-1}, which is much smaller compared to the spread of radial velocity caused by Galactic differential rotation. The relatively narrow width of the lines indicate that the line emitting region is not spread out along the line of sight. A region with a low filling factor and confined to small regions along the line of sight cannot be considered as a distributed medium. We therefore conclude that the low-density ionized gas responsible for the RRL emission does not form a pervasive medium as suggested by the term ELDWIM.

In the morphological model proposed by Petuchowski & Bennett (1993) for the ELDWIM, the two observationally distinct distributions of the ionized gas (i.e., the WIM and the low-density ionized gas) are conflated. According to this model, the rms electron density $\langle n_e^2 \rangle^{0.5}$ of the WIM becomes large enough in the inner Galaxy to produce observable RRL emission. If this is true, then we expect the distribution of the RRL emitting gas to be similar to that of the WIM. As discussed in § 4.2, any comparison of the distribution of these ionized gases in the inner Galaxy is complicated by the facts that Hα photons suffer large interstellar extinction and the sensitivity of existing RRL observations may not be adequate to detect the WIM in the inner Galaxy. Thus, "WIM in the inner Galaxy produces observable RRL emission" remains only a conjecture and does not (yet) have any observational evidence.

There are three other difficulties with the ELDWIM model. As described above, the O stars producing the low-density ionized gas are thought to evolve beyond the H II region phase and, hence, not to have any associated dense ionized gas. However, McKee & Williams (1997) argue that it is difficult to disperse the dense gas, from which the massive stars are formed, during the lifetime ($\sim 4 \times 10^6$ yr; Williams & McKee 1997) of the stars responsible for most of the ionization.

The second difficulty concerns the spectrum of the ionizing radiation. Using RRL observations near 1.4 GHz, Heiles et al. (1996a) have obtained constraints on the required spectrum of the ionizing radiation for the ELDWIM. They showed that it is difficult to generate the spectrum of the ionizing photons from the current models of star formation, which they refer to as the ionizing-spectrum problem. Heiles et al. (1996a) have inferred this spectrum from the measured ratio of ionized helium to hydrogen (n_{He^+}/n_{H^+}) from their RRL observations. The upper limit to this ratio measured from the RRL observations near 1.4 GHz is $\sim$0.013 (Heiles et al. 1996a). This ratio corresponds to an upper limit on the helium ionization fraction of $\sim$0.13 if we assume that the hydrogen is fully ionized in the ELDWIM. Such a small ionization fraction can be achieved in H II regions if the ionizing radiation field is produced by massive stars with temperatures less than 35,000 K (equivalent to an O7 star; Osterbrock 1989). From our current knowledge of the initial mass function and the total Galactic star formation rate, it is difficult to simultaneously obtain the required ionizing radiation field

and the total ionization requirement for the WIM and the H II regions (Heiles et al. 1996a).

Finally, the hot stars that are required to ionize the ELDWIM are usually considered to produce locally confined ionized regions (H II regions). In contrast, the ELDWIM is pervasive and widely distributed. Heiles et al. (1996a) argue that this pervasiveness leads to the difficulty that the photons from the hot stars have to travel long distances to ionize the ELDWIM, which they refer to as the morphological problem.

In summary, the ELDWIM has difficulty in explaining (1) the association of RRL emission near 327 MHz with the star-forming region, (2) the low filling factor obtained from the derived physical properties for the low-density ionized gas, and (3) the observed typical low-frequency recombination line width of 30 km s^{-1}. We conclude that the ELDWIM model does not portray the origin of RRL emitting low-density ionized gas in the inner Galaxy.

5.3. *Low-density Envelopes of* H II *Regions*

An alternate model for the origin of low-density ionized gas is that it forms the large, low-density envelopes of normal H II regions. This hypothesis was proposed by Anantharamaiah (1986) based on his RRL observations with longitudes $l < 45°$. In this longitude range, the number of normal, higher density H II regions is large (~ 700) compared to that of other regions of the Galaxy. Anantharamaiah (1986) argued that if these H II regions have low-density envelopes of size ~ 100 pc, then practically every line of sight in this longitude range will intercept at least one of them, thus explaining the ubiquity of low-frequency RRL emission within $l < 45°$. The data in Paper I indicates that the H II–envelope model can be further extended to explain the line emission in the longitude range $l = 330°$ to 0° to 89° since a good degree of similarity is seen between the distribution of RRL emission near 327 MHz in this longitude range and that of the star-forming region as indicated by "intense" ^{12}CO and high-frequency RRLs from normal H II regions. Furthermore, there is no observational bias in our data since the 327 MHz survey forms a complete sampling of the inner Galaxy.

The H II–envelope model for the origin of the low-density ionized gas naturally explains some of the other observed features. The large fluctuations seen in line emission as a function of longitude can be expected in this model since the line-of-sight intercepts H II envelopes of different physical properties. The filling factor estimated for the low-density gas from our data is reasonable for the H II–envelope model as the ionized gas responsible for line emission are individual objects of size 20–200 pc and thus will not form a pervasive medium as proposed by the ELDWIM model. The large scale height (~ 100 pc) derived for the observed RRL emission near 327 MHz compared to that of the H II regions is also expected in the H II–envelope model since the sizes of the low-density envelopes (20–200 pc) are larger than the typical sizes of H II regions (1–10 pc). The detection of RRLs in almost all positions in the higher resolution observations near 327 MHz, toward fields with $l < 35°$ (Paper II), and comparatively fewer number of lines observed toward fields with $l > 35°$ can be understood in this model as follows. About 75% of H II regions identified in high-frequency RRL surveys toward continuum sources are in the longitude range $l = 0°$ to 35° ($|b| < 1.°5$). The average separation between H II regions in this longitude is $\sim 0.°08$ compared to $\sim 0.°3$ in the longitude range $l = 35°$ to 85°. Considering that more than 50% of the estimated sizes of the low-density ionized gas are between 20 and 100 pc and assuming a distance to the ionized gas as 5 kpc, the average angular size of the H II envelope is $\sim 0.°5$. If we assume that most of the H II regions have an associated low-density envelope, then the probability of almost every line of sight in the longitude range $l = 0°$ to 35° intersecting at least one H II envelope is high. This probability is reduced in the longitude range $l = 35°$ to 85° because of larger angular separation between the H II regions. A similar argument can explain the lack of widespread emission of lines in the outer Galaxy since the number density of H II regions in the outer Galaxy is much less compared to that of the inner Galaxy.

There are direct observations which provide evidence for the association of large, low-density gas formations with normal H II regions. Analysis of the H166α observations from W3, W4, and W5 H II region complexes by Hart & Pedlar (1976a) shows the presence of low-density ionized gas that is associated with the H II regions. Recent observations of RRLs near 1.4 GHz by Heiles et al. (1996b) have detected lines that are attributed to walls of cavities in the galactic gaseous disk formed by clustered supernovae. These walls, which are termed "worms" by Heiles et al. (1996b), are ionized by photons from the hot stars in the cluster the supernovae of which created the cavity. Heiles et al. (1996b) estimated that about 17% of the observed low-frequency RRL emission originates in these "worms." Most of the OB associations, to which a worm can be associated with, do indeed have radio H II regions. Thus, as pointed out by McKee & Williams (1997), worms can also be classified in the H II–envelope picture, in that they are also generated by ionizing photons that escape from the density-bounded H II regions. A recent low-frequency continuum observation of Orion A shows the presence of low-density ionized gas associated with the H II region (Subrahmanyan, Goss, & Malin 2001), a further support for the H II–envelope picture.

Association of a large, low-density component with normal H II regions is also indicated by a recent study of the luminosity function of OB associations in the Galaxy (McKee & Williams 1997). For this study, McKee & Williams (1997) considered two main possibilities—(1) there are more OB associations in the Galaxy than are observed as radio H II regions with the remainder being "extended low-density" H II regions (Mezger 1978); (2) the radio H II regions are partially density bounded and, hence, have an associated low-density envelope that is not bright in radio continuum. Comparing the luminosity distribution of H II regions in the Galaxy with that of other galaxies, McKee & Williams (1997) concluded that the H II–envelope picture is a better representation of the OB association in the Galaxy. This conclusion is consistent with the suggestion by Anantharamaiah (1986) and further supported by the data in Papers I & II.

The H II–envelope model offers a natural resolution to two of the three problems encountered by the ELDWIM model that were mentioned before. As described above, in the H II–envelope model, the low-density ionized gas is physically associated with normal, higher density H II regions. Thus, in this model it is not required to disperse the dense ionized gas during the lifetime of the stars, as is needed by the ELDWIM model. For the same reason, the ionizing photons need not travel long distances from the

hot stars to produce the low-density ionized gas, thus resolving the morphological problem of the ELDWIM model.

In summary, the H II–envelope model explains the association of low-density ionized gas with normal, higher density H II regions as indicated by the 327 MHz RRL data (Paper I). The model also accounts for (1) the low filling factor of the low-density gas, (2) large fluctuations observed in line emission as a function of longitude in the inner Galaxy, and (3) lack of widespread emission of lines in the outer Galaxy. In view of these and other evidence presented above, we conclude that the low-density envelopes of H II regions are the favored site for the origin of RRL emission observed near 327 MHz.

5.4. *A Population of Evolved, Large, Low-density H II Regions*

Mathews et al. (1973) have used RRL and continuum emission near 1.4 GHz in the longitude range $l < 48°$ to estimate the properties of the ionized gas producing RRLs. They derived temperature and density for the line emitting region as $\sim$6000 K and $\sim$2 cm^{-3}, respectively. These regions have an angular extent of $\sim 3°$–$5°$. Based on these estimates, they suggested that the ionized gas responsible for low-frequency RRL emission are extended low-density H II complexes similar to NGC 2244, NGC 7000, and NGC 7822. Multifrequency centimeter-wave RRL observations toward a set of directions in the inner Galaxy were used by Shaver (1976) to constrain the physical properties of the ionized gas producing line emission. Analysis of these observations indicated that in most cases the ionized gas should have electron densities of 5–10 cm^{-3} and diameters of 20–150 pc with relatively high temperature (greater than a few 1000 K). Based on these derived parameters, Shaver (1976) also suggested that the gas responsible for line emission were the large low-density H II regions.

A large population of evolved, low-density H II regions in the inner Galaxy can explain many of the properties of RRL emission near 327 MHz. There is no physical reason for the evolved H II region to have a different spatial distribution in the Galactic disk compared with those of compact H II regions. Thus, similarity of the distribution of RRL emission near 327 MHz with the star-forming region is expected in this model as well. This argument also explains the lack of the line emission in the outer Galaxy. The low filling factor deduced from the estimated physical properties of RRL emitting gas is also expected in this model as the line emission originates in individual, evolved H II regions. For the same reason, the expected line widths do not have contribution from Galactic differential rotation; hence, a typical line width of 30 km s^{-1} for the detected RRL near 327 MHz is reasonable. Thus, we conclude that an ensemble of evolved, low-density H II regions in the inner Galaxy as a model for the origin of low-frequency RRL cannot be ruled out from the existing data.

6. SUMMARY

An extensive set of observations of RRLs in the Galactic plane, at a frequency near 327 MHz were made by Roshi & Anantharamaiah (2000, 2001) using the Ooty Radio Telescope (ORT). This paper concerns the estimation of the physical properties of the ionized gas responsible for RRL emission near 327 MHz. The derived electron densities of the ionized gas are in the range 1–10 cm^{-3}. The upper limits obtained for the temperatures and sizes of the line emitting regions are typically $T_e \sim$ 12,000 K and $S \sim$ 500 pc. The path lengths through the regions, assuming an electron temperature of 7000 K, are in the range 20–200 pc.

Using the derived physical properties, we estimated the expected [C II] 158 μm and [N II] 205 μm line emission from these low-density ionized regions. Most of the [N II] emission and a considerable fraction of the [C II] emission observed by the *COBE* satellite could originate in the same ionized gas that is responsible for the RRL emission. The Hα emission from these ionized gases is mostly not detected in the existing Hα surveys because of large interstellar extinction. We also computed the expected free-free absorption of the Galactic nonthermal emission near 34.5 MHz because of the presence of these ionized clouds. About 50% of the absorption of the background radiation at frequencies less than 100 MHz could be caused by the low-density ionized gas.

We also discussed the origin of low-density ionized gas in the context of three of the existing models—the ELDWIM model, the H II–envelope model, and an ensemble of evolved, low-density H II regions. On the basis of the similarity of the distribution of the RRL emission in the Galactic disk with that of the star-forming regions and the range of derived physical properties, we have suggested that the RRL emission originates from low-density ionized gas that forms envelopes of normal H II regions. Our estimated filling factor for the low-density ionized gas is less than 1%. This low filling factor indicates that the ionized gas does not form a pervasive medium as suggested by the term "extended low-density warm ionized medium" (ELDWIM) that has been used in the literature to describe this component. However, the origin of low-frequency RRL emission from an ensemble of evolved, low-density H II regions cannot be ruled out from the existing data.

We thank A. Pramesh Rao, Jayaram N. Chengalur, and Gopal Krishna for many discussions and helpful suggestions. We thank E. Fürst and T. Handa for providing the continuum maps of the Galactic plane. This work forms a part of the Ph.D. thesis of D. A. R.

REFERENCES

Altenhoff, W. J., Downes, D., Pauls, T., & Schraml, J. 1979, A&AS, 35, 23
Anantharamaiah, K. R. 1985a, J. Astrophys. Astron., 6, 177
———. 1985b, J. Astrophys. Astron., 6, 203
———. 1986, J. Astrophys. Astron., 7, 131
Broadbent, A., Osborne, J. L., & Haslam, C. G. T. 1989, MNRAS, 237, 381
Brocklehurst, M., & Salem, M. 1977, Comput. Phys. Commun., 13, 39
Burton, W. B., & Gordon, M. A. 1978, A&A, 63, 7
Caswell, J. L., & Haynes, R. F. 1987, A&A, 171, 261
Cersosimo, J. C. 1990, ApJ, 349, 67
Combes, F. 1991, ARA&A, 29, 195
Dwarakanath, K. S. 1989, Ph.D thesis, Indian Institute of Science
Dwarakanath, K. S., & Udaya Shankar N. 1990, J. Astrophys. Astron., 11, 323
Erickson, W. C., McConnell, D., & Anantharamaiah, K. R. 1995, ApJ, 454, 125
Gordon, M. A., & Cato, T. 1972, ApJ, 176, 587
Gottesman, S. T., & Gordon, M. A. 1970, ApJ, 162, L93
Hakkila, J., Myers, J. M., Stidham, B. J., & Hartmann, D. H. 1997, AJ, 114, 2043
Handa, T., Sofue, Y., Nakai, N., Hirabayashi, H., & Inoue, M. 1987, PASJ, 39, 709
Hart, L., & Pedlar, A. 1976a, MNRAS, 176, 135

Hart, L., & Pedlar, A. 1976b, MNRAS, 176, 547
Haslam, C. G. T., Stoffel, H., Salter, C. J., & Wilson, W. E. 1982, A&AS, 47, 1
Heiles, C. 1994, ApJ, 436, 720
Heiles, C., Koo, B.-C., Levenson, N. A., & Reach, W. T. 1996a, ApJ, 462, 326
Heiles, C., Reach, W. T., Koo, B.-C. 1996b, ApJ, 466, 191
Kerr, F. J., & Lynden-Bell, D. 1986, MNRAS, 221, 1023
Kulkarni, S. R., & Heiles, C. 1988, in Galactic and Extragalactic Radio Astronomy, ed. G. H. Verschuur & K. I. Kellermann (Berlin: Springer), 95
Lockman, F. J. 1976, ApJ, 209, 429
———. 1980, in Radio Recombination Lines, ed. P. A. Shaver (Dordrecht: Reidel), 185
———. 1989, ApJS, 71, 469
Lockman, F. J., Pisano, D. J., & Howards, G. J. 1996, ApJ, 472, 173
Matthews, H. E., Pedlar, A., & Davies, R. D. 1973, MNRAS, 165, 149
McKee, C. F., & Ostriker, J. P. 1977, ApJ, 218, 148
McKee, C. F., & Williams, J. P. 1997, ApJ, 476, 144
Mezger, P. G. 1978, A&A, 70, 565
Nakagawa, T., et al. 1998, ApJS, 115, 259
Osterbrock, D. E. 1989, Astrophysics of Gaseous Nebulae and Active Galactic Nuclei (Mill Valley: University Science Books)
Payne, H. E., Anantharamaiah, K. R., & Erickson, W. C. 1994, ApJ, 430, 690
Petuchowski, S. J., & Bennett, C. L. 1993, ApJ, 405, 591
Reich, W., Fürst, E., Reich P., & Reif, K. 1990, A&AS, 85, 633
Reynolds, R. J. 1983, ApJ, 268, 698
Rodgers, A. W., Campbell, C. T., & Whiteoak, F. B. 1960, MNRAS, 121, 103
Roshi, A. D., & Anantharamaiah, K. R. 2000, ApJ, 535, 231 (Paper I)
———. 2001, J. Astrophys. Astron., 22, 81 (Paper II)
Salter, C. J., & Brown, R. L. 1988, in Galactic and Extragalactic Radio Astronomy, G. H. Verschuur & K. I. Kellermann (Berlin: Springer), 1
Shain, C. A., Komesaroff, M. M., & Higgins, C. S. 1961, Australian J. Phys., 14, 508
Shaver, P. A. 1975, Pramana, 5, 1
———. 1976, A&A, 49, 1
Shaver, P. A., McGee, R. X., Newton, L. M., Danks, A. C., & Pottasch, S. R. 1983, MNRAS, 204, 53
Shaver, P. A., McGee, R. X., & Pottasch, S. R. 1979, Nature, 280, 476
Sivan, J. P. 1974, A&AS, 16, 163
Smith, L. F., Biermann, P., & Mezger, P. G. 1978, A&A, 66, 65
Solomon, P. M., Sanders, D. B., & Rivolo, A. R. 1985, ApJ, 292, L19
Subrahmanyan, R., Goss, W. M., & Malin, D. F. 2001, AJ, 121, 399
Swarup, G., et al. 1971, Nature Phys. Sci., 230, 185
Taylor, J. H., & Cordes J. M. 1993, ApJ, 411, 674
Walmsley, C. M., & Watson, W. D. 1982, ApJ, 260, 317
Westerhout, G. 1958, Bull. Astron. Inst. Netherlands, 14, 215
Williams, J. P. & McKee, C. F. 1997, ApJ, 476, 166
Wood, D. O. S., & Churchwell, E. 1989, ApJS, 69, 831
Wright, E. L., et al. 1991, ApJ, 381, 200